ACS OMEGA

Open Access

http://pubs.acs.org/journal/acsodf

Article

Advocating the Use of Bayesian Network in Analyzing the Modes of Occurrence of Elements in Coal

Na Xu,* Qiang Li, Wei Zhu, Qing Li, Robert B. Finkelman, Mark A. Engle, Ru Wang, and Zhiwei Wang

Cite This: *ACS Omega* 2023, 8, 39096−39109

Read Online

ACCESS | Metrics & More | Article Recommendations

ABSTRACT: Modes of occurrence of elements in coal are important because they can be used not only to understand the origin of inorganic components in coal but also to determine the impact on the environment and human health and the deposition process of coal seams as well. Statistical analysis is one of the commonly used indirect methods used to analyze the modes of occurrence of elements in coal, among which hierarchical clustering is widely used. However, hierarchical clustering may lead to misleading results due to its limitation that it focuses on the clusters of elements rather than a single element. To tackle this issue, we use the first part of a well-known Bayesian network structure learning algorithm, i.e., Peter−Clark (PC) algorithm, to explore the relationships of the coal elemental data and then infer modes of occurrence of elements in coal. A data set containing 95 Late Paleozoic coal samples from the Datanhao and Adaohai mines in Inner Mongolia, China, is used for the performance evaluation. Analytical results show that many instructive and surprising insights can be concluded from the first part of the PC algorithm. Compared with the hierarchical clustering algorithm, the first part of the PC algorithm demonstrates superiority in analyzing the modes of occurrence of elements in coal.

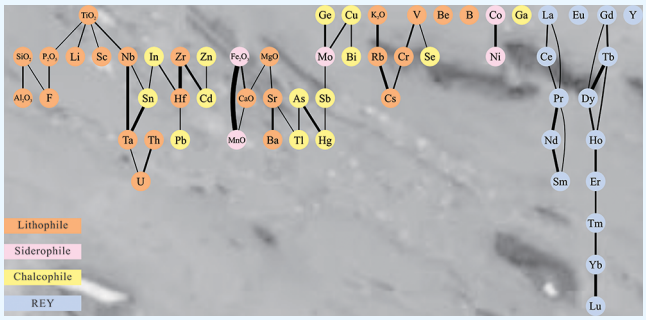

1. INTRODUCTION

Coal is an important nonrenewable resource. Almost every nongaseous element has been found in coal.[1] It is of great significance to accurately analyze the modes of occurrence of elements in coal because: (1) they can be used to infer the origin of minerals in coal and the geological process of coal formation;[1−3] (2) they can provide useful information for the recovery of critical elements, such as rare earth elements (REE), Ge, Ga, and U, from coal and coal combustion products;[4−6] (3) they are also helpful to solve many technical problems encountered in mining, processing, and coal utilization;[7,8] and (4) understanding the modes of occurrence of toxic elements (e.g., As, Hg, and Se) in coal can diminish serious impacts on the environment and human health.[1,9,10]

There are two categories of analytical methods for determining the modes of occurrence of elements in coal: direct and indirect methods.[1,11] Direct methods include laser ablation-inductively coupled plasma-mass spectrometry (LA-ICP-MS), electron microprobe analysis (EMPA), scanning electron microscopy with energy-dispersive X-ray spectroscopy (SEM-EDS), X-ray diffraction (XRD), X-ray fluorescence spectrometry (XRF), X-ray photoelectron spectroscopy, transmission electron microscopy, sensitive high-resolution ion microprobe, proton-induced X-ray emission, optical microscopy, etc. Indirect methods include float-sink methods, selective leaching, and statistical analysis methods (e.g., correlation analysis, cluster analysis, and principal component analysis).[1,11] Among the statistical analysis methods, agglomerative hierarchical clustering is commonly used. It initially treats each element as a single cluster, then calculates the distance between different clusters, and merges the two closest clusters to form a new cluster at each clustering stage. This process is repeated until a complete clustering tree is formed.[12] Denoting the coal elemental data as a vector $\boldsymbol{X} = [x^{(1)}, x^{(2)}, \cdots, x^{(n)}]$, and single element as $x^{(i)} = [x_1^{(i)}, x_2^{(i)}, \cdots, x_m^{(i)}]^T$, $i = 1 \cdots n$, where m and n are the sample size and element number, respectively, then the similarity between element $x^{(i)}$ and element $x^{(j)}$ can be denoted as $D(x^{(i)}, x^{(j)})$. Pearson correlation is commonly used to measure the similarity between two elements. Xu et al.[13,14] demonstrated that the agglomerative hierarchical clustering based on the average-linkage principle is significantly better than those based on complete linkage, single linkage, and centroid linkage. Average linkage denotes the average distance between elements of two different clusters, which can be expressed as

Received: June 10, 2023
Accepted: September 21, 2023
Published: October 10, 2023

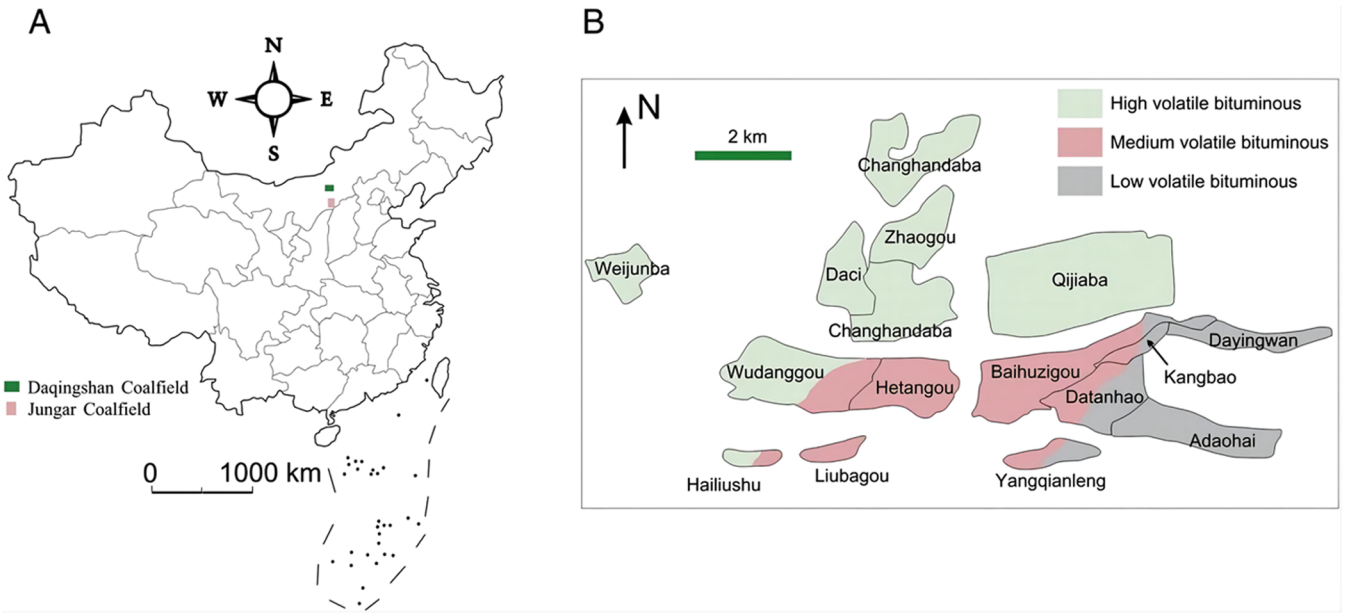

Figure 1. Location of the Daqingshan Coalfield (A) and coal rank distribution in the different mines of the coalfield (B). Reprinted with permission from ref 23. Copyright 2012 Elsevier.

$d(C_p, C_q) = \sum_{x^{(i)} \in C_p} \sum_{x^{(j)} \in C_q} \frac{D(x^{(i)}, x^{(j)})}{|C_p||C_q|}$, where $|C_p|$ and $|C_q|$ represent the count of elements in clusters C_p and C_q, respectively.

However, such a hierarchical clustering algorithm has a disadvantage; i.e., it focuses on the clusters of multiple elements rather than a single element; once an initial cluster is clustered wrongly, the subsequent clustering process may further lead to wrong results that cannot be reasonably explained. Therefore, it is not accurate to analyze the modes of occurrence of elements belonging to different clusters.

Bayesian network is one of the common machine learning models with broad applications in different fields of artificial intelligence, including causal inference, uncertain knowledge expression, and pattern recognition.[15−20] Parameter learning and structure learning are two components of Bayesian network learning, with structure learning being its core part. Structure learning is the core part that can learn the relationships between vertices from the given data set.[21,22]

In this paper, we focus on the application of the Bayesian network to analyze the modes of occurrence of elements in coal and advocate the use of the first part of the Peter−Clark (PC) algorithm, a Bayesian network structure learning algorithm to explore the associations of coal elemental data. Samples used in this study are from the Datanhao and Adaohai mines in the Daqingshan Coalfield, Inner Mongolia, China. The results obtained by the first part of the PC algorithm are more reliable and more consistent with the geochemical principles than the results of the aforementioned hierarchical clustering algorithm. The accuracy of the results has been validated with previous investigations and their geochemistry nature.

2. GEOLOGICAL SETTING AND SAMPLE DATA

Samples used in this study were collected from the Datanhao and Adaohai mines in the Daqingshan Coalfield in Inner Mongolia, China (Figure 1). The Daqingshan Coalfield contains 16 mines, with the Datanhao and Adaohai mines located southeast of the coalfield (Figure 1B). The coal-bearing strata in the Daqingshan Coalfield include the Pennsylvanian Shuanmazhuang Formation and the Early Permian Zahuaigou Formation,[23] and the main mineable coalbed is the Late Paleozoic coal (i.e., CP2 coal) located in the upper portion of the Shuanmazhuang Formation. The coalbed has a thickness varying from 4.72 to 42.79 m, with an average of 22.58 m. The roof of the coalbed has a variable thickness and mainly consists of mudstone and sandy mudstone.[23] Also, both the thickness and lithology of its floor vary considerably with a thickness from 0.2 to 2.0 m and a lithological composition of sandy sandstone, medium-coarse sandstone, and fine sandstone.[23] The coal rank in the Daqingshan Coalfield ranges from high volatile bituminous coal and medium volatile bituminous coal to low volatile bituminous coal from northwest to southeast (Figure 1B) due to the influence of igneous intrusion.[23,24]

A total of 62 samples from the CP2 coal of the Datanhao mine were collected by Zhao et al.,[25] which are divided into three categories, including 20 coal benches, 40 partings, and 2 roof strata samples. In addition, a total of 48 samples from the CP2 coal of the Adaohai mine were collected by Dai et al.,[23] which are also divided into three categories, including 33 coal benches, 11 partings, and 4 roof samples. Our focus in this paper is on the 62 samples of the Datanhao mine and the 33 coal bench samples of the Adaohai mine. According to Zhao et al.,[25] XRF was used to determine the contents of major-element oxides after all of the 62 samples were ashed at 815 °C. Samples (particle size < 1 mm) were also examined in a polished section using SEM-EDS techniques, to identify the modes of mineral occurrence. ICP-MS was used to determine the concentration of most trace elements in all samples and arsenic as well. In addition, ICP-MS with collision cell technique was used to analyze the arsenic and selenium in the samples. According to Dai et al.,[23] optical microscopic observation and powder XRD are used to determine the mineralogy. Vario MACRO (an elemental analyzer) was used to determine the percentages of C, H, and N in the coal. XRF was used to determine the oxides of major elements for the coal ash (815 °C), including SiO_2, Al_2O_3, CaO, K_2O, Na_2O, Fe_2O_3, MnO, MgO, TiO_2, and P_2O_5, and

https://doi.org/10.1021/acsomega.3c04109
ACS Omega 2023, 8, 39096−39109

Table 1. PC-Skeleton Algorithm[a]

Input: Conditional independence information among all elemental vertices in V, an ordering order(V) on the elemental vertices

Output: Estimated skeleton C

Form the complete undirected graph $\tilde{C}$ on the elemental vertices set V.

$\ell = -1, C = \tilde{C}$

repeat

$\ell = \ell + 1$

for all elemental vertices $v^{(i)}$ in C **do**

Let $\boldsymbol{a}(i) = \boldsymbol{Adjacent}(C, i)$

end for

repeat

Select a (new) ordered pair of elemental vertices $(v^{(i)}, v^{(j)})$ that are adjacent in C and satisfy $|\boldsymbol{a}(i)\backslash\{j\}| \geq \ell$, using order($V$)

repeat

Choose a (new) set $\boldsymbol{k} \subseteq \boldsymbol{a}(i)\backslash\{j\}$ with $|\boldsymbol{k}| = \ell$, using order(V)

if $v^{(i)}$ and $v^{(j)}$are conditionally independent given $\boldsymbol{k}$ then

Delete edge $(v^{(i)}, v^{(j)})$ from C

end if

until $v^{(i)}$ and $v^{(j)}$ are no longer adjacent in C or all $\boldsymbol{k} \subseteq \boldsymbol{a}(i)\backslash\{j\}$ with $|\boldsymbol{k}| = \ell$ have been considered

until all ordered pairs of adjacent elemental vertices $(v^{(i)}, v^{(j)})$ in C with $|\boldsymbol{a}(i)\backslash\{j\}| \geq \ell$ have been considered

until all pairs of adjacent elemental vertices $(v^{(i)}, v^{(j)})$ in C satisfy $|\boldsymbol{a}(i)\backslash\{j\}| \leq \ell$.

[a]Reprinted in part with permission from ref 28,32. Copyright 2007, 2014 Microtome Publishing.

arsenic as well. ICP-MS was used to determine trace elements in the coal samples except for Hg, F, and Cl. In addition, the permeability of mercury was determined using a Milestone DMA-80 Hg analyzer. Fluorine and Cl were determined by pyrohydrolysis with an ion-selective electrode.

According to Zhao et al.[25] and Dai et al.,[23] Datanhao coal and Adaohai coal belong to medium volatile bituminous coal and low volatile bituminous coal, respectively. In addition, both Datanhao (0.51% total sulfur on average, dry basis) and Adaohai (0.78% total sulfur on average, dry basis) coals are low-sulfur coals (coals with total sulfur content <1%).[23,25] The Datanhao mine is not far from the Adaohai mine (Figure 1B) but the nature of their coals is very different. Compared with common Chinese coals, the Datanhao coal has high concentrations of Al_2O_3, SiO_2, TiO_2, CaO, and MnO (on whole-coal basis).[10,25] In addition, compared with world hard coals as reported by Ketris and Yudovich,[26] the CP2 coal of the Datanhao mine is rich in Zr, Hf, Th, Be, F, Zn, Ga, Nb, Mo, Cd, In, Sn, Ta, Hg, Pb, and rare earth elements and yttrium (REY), but the content of Li, B, Cr, Ni, As, Rb, Sr, Cs, and Tl is lower.[25] Compared with common Chinese and world coals as reported by Dai et al., the CP2 coal of the Adaohai mine is rich in CaO, MgO, P_2O_5, F, Ga, Zr, Ba, Hg, Pb, and Th but has a lower SiO_2/Al_2O_3 ratio.[23,26] Tables in the supplementary materials list the concentrations of major oxides, trace elements, and REY of samples from Datanhao mine and Adaohai mine, respectively.

https://doi.org/10.1021/acsomega.3c04109
ACS Omega 2023, 8, 39096−39109

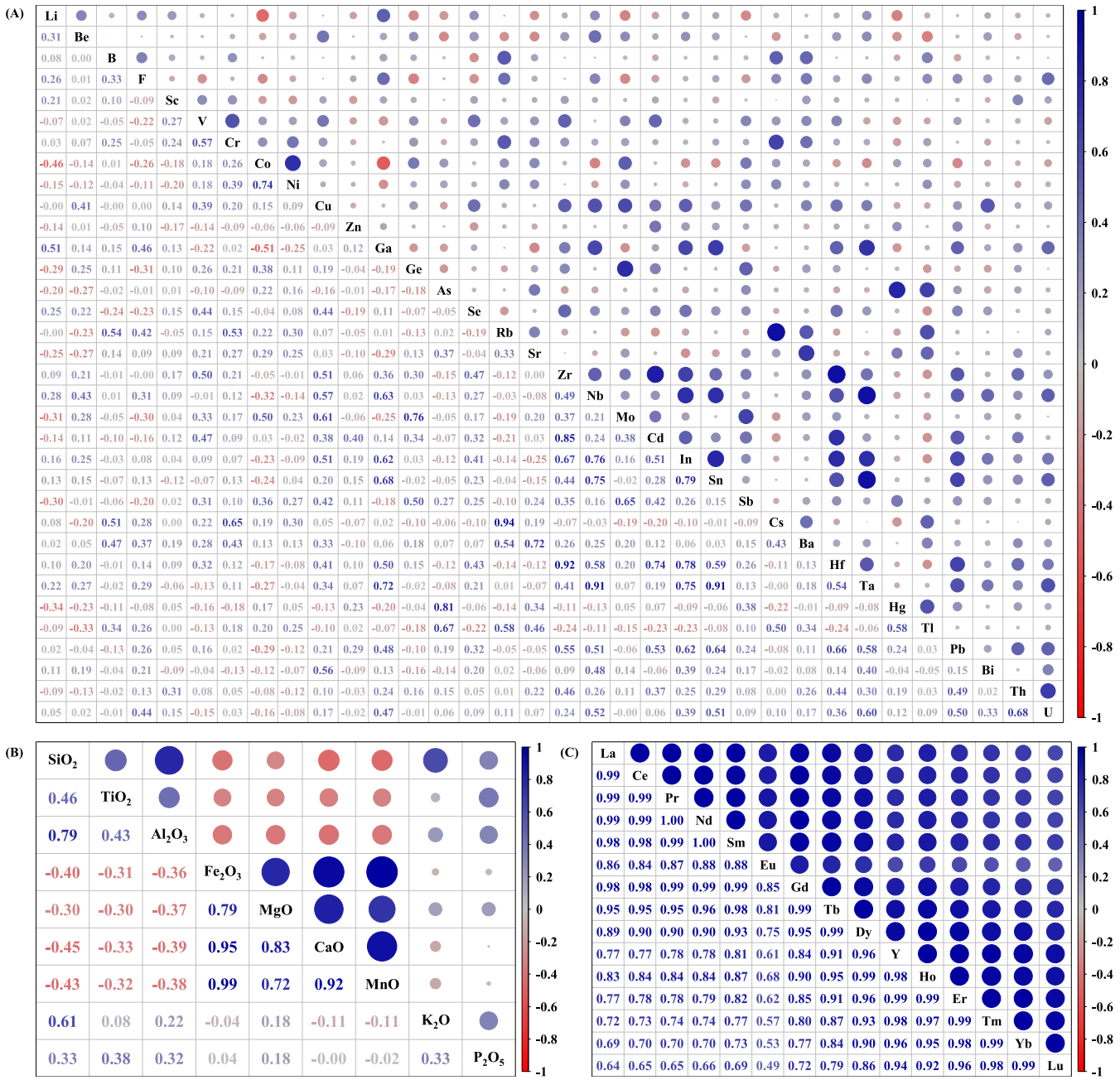

Figure 2. Pearson correlation coefficients between elements in the Datanhao coal. (A) Trace elements; (B) major elements; and (C) REY.

3. METHOD

The Bayesian network structure is a directed acyclic graph which consists of vertices and directed edges.[27] The undirected graph obtained from a directed acyclic graph G by replacing directed edges with undirected edges is the skeleton of G that encodes the conditional independence relations of vertices.[28] Bayesian network structure learning algorithms can be used to learn the network structure of the given data set.[29−31]

The PC algorithm is a well-known algorithm for learning the structure of Bayesian networks. Since its learning result is reliable when dealing with sparse graphs with many variables, it can be used for learning the Bayesian network structure in high-dimensional cases,[28,32] which is suitable for analyzing coal elemental data. The PC algorithm mainly includes two components: estimating the skeleton and partially orienting the edges. In this study, we use the first part (hereafter referred to as the PC-skeleton algorithm) to obtain the skeleton of the given coal elemental data.

Let the set of vertices $[\boldsymbol{V} = v^{(1)}, v^{(2)}, \cdots, v^{(n)}]$ correspond to the coal elemental data $\boldsymbol{X} = [x^{(1)}, x^{(2)}, \cdots, x^{(n)}]$, and each vertex $v^{(i)}$ correspond to $x^{(i)}$. The set of edges representing associations of elements can be expressed as $E \subseteq V \times V$ (i.e., the edge set is a subset of ordered pairs of distinct vertices). Bayesian network structure learning algorithm can be used to obtain the skeleton of directed acyclic graph $G = (V, E)$ based on the coal elemental data. Let M, N, and W be three disjoint subsets of vertices in G, W is said to d-separate M from N, if along every path between a vertex in M and a vertex in N there is vertex w satisfying one of the following two conditions: (1) w has converging arrows and none of w or its descendants are in W, or (2) w does not have converging arrows and w is in W.[27] The adjacency set of the elemental vertex $v^{(i)}$ in G, denoted by ***Adjacent***(G, i), are all

https://doi.org/10.1021/acsomega.3c04109
ACS Omega 2023, 8, 39096−39109

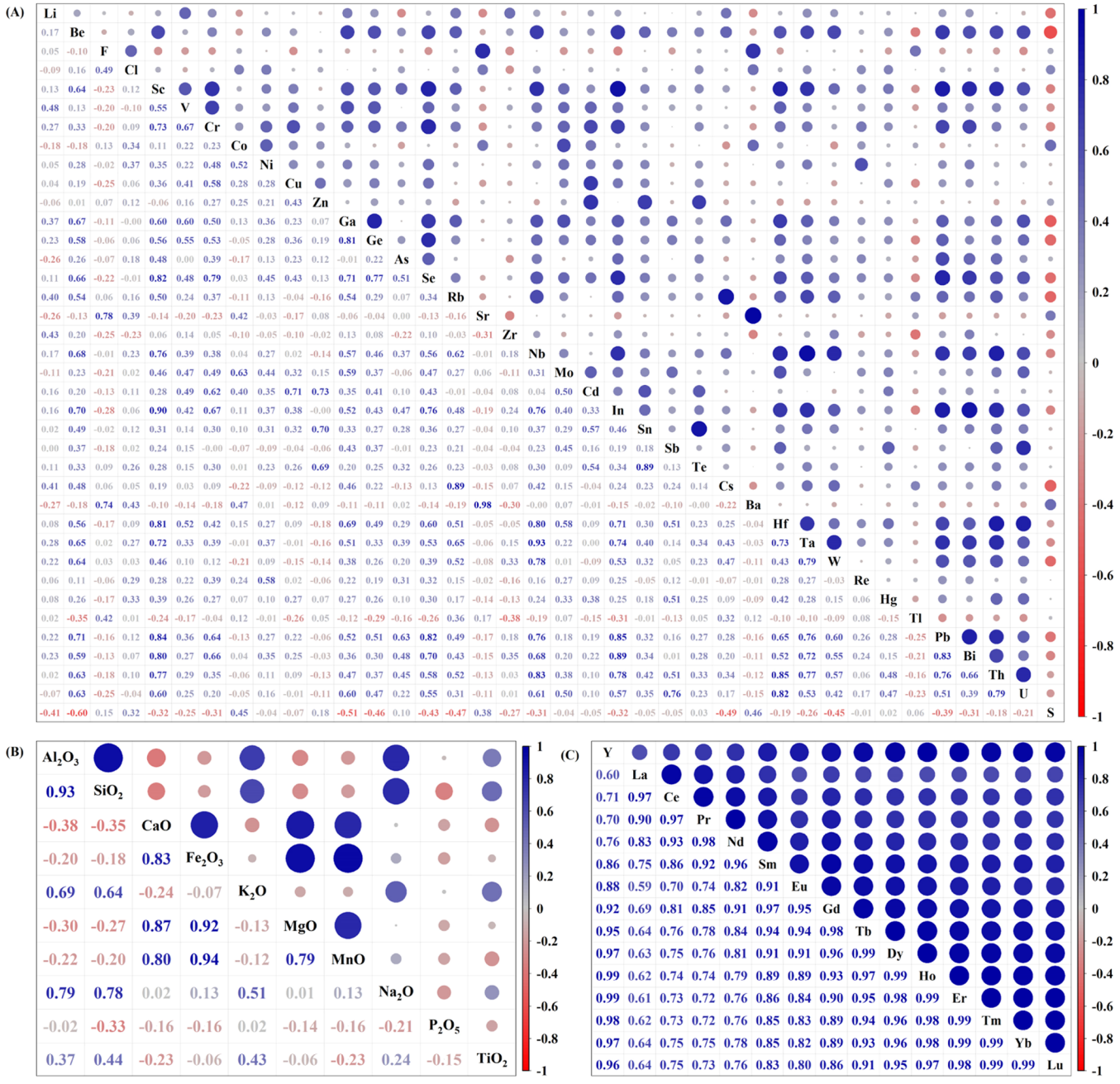

Figure 3. Pearson correlation coefficients between elements in the Adaohai coal: (A) Trace elements; (B) major elements; and (C) REY.

elemental vertices which are directly connected to $v^{(i)}$ by an edge (directed or undirected). The elements of ***Adjacent***(G, i) are also called neighbors of (or adjacent to) $v^{(i)}$. The core idea of the PC-skeleton algorithm is to first perform conditional independence tests and then construct a skeleton that covers as many conditional independencies as possible. After each new size l of the conditioning sets is updated, the algorithm stores the adjacency set ***Adjacent***(G, i) of all elemental vertices. These stored adjacency sets are used whenever the algorithm searches for conditioning sets of given size l. Consequently, an edge deletion has no effect on which conditional independencies are tested for other pairs of elemental vertices at this level of l.[32] Specifically, when analyzing the modes of occurrence of elements in coal, each element represented by a vertex has its own geochemical meaning and operates independently in each iteration of structure learning. This is an advantage that hierarchical clustering algorithms do not possess and is the reason that hierarchical clustering algorithms can produce misleading results. A skeleton of Bayesian network structure can be obtained at the end of the PC-skeleton algorithm execution.[28,32]

Assume the distribution P of the coal elemental data $\boldsymbol{X}$ is a multivariate normal. For a given directed acyclic graph G, the distribution P is faithful to G implying that the conditional independence relations correspond to d-separations and vice versa.[28] For $i \neq j \in \{1, \cdots, n\}$, $\boldsymbol{k} \subseteq \{1, \cdots, n\} \backslash \{i, j\}$, $\rho_{i, j|\boldsymbol{k}}$ denotes the partial correlation between $\boldsymbol{x}^{(i)}$ and $\boldsymbol{x}^{(j)}$ given $\{\boldsymbol{x}^{(r)}; r \in \boldsymbol{k}\}$. Then, $\rho_{i, j|\boldsymbol{k}} = 0$ if and only if $\boldsymbol{x}^{(i)}$ and $\boldsymbol{x}^{(j)}$ are conditionally independent given $\{\boldsymbol{x}^{(r)}; r \in \boldsymbol{k}\}$.[33] The PC-skeleton algorithm (Table 1) thus can estimate partial correlations to obtain estimations of conditional independencies. The partial

https://doi.org/10.1021/acsomega.3c04109
ACS Omega 2023, 8, 39096−39109

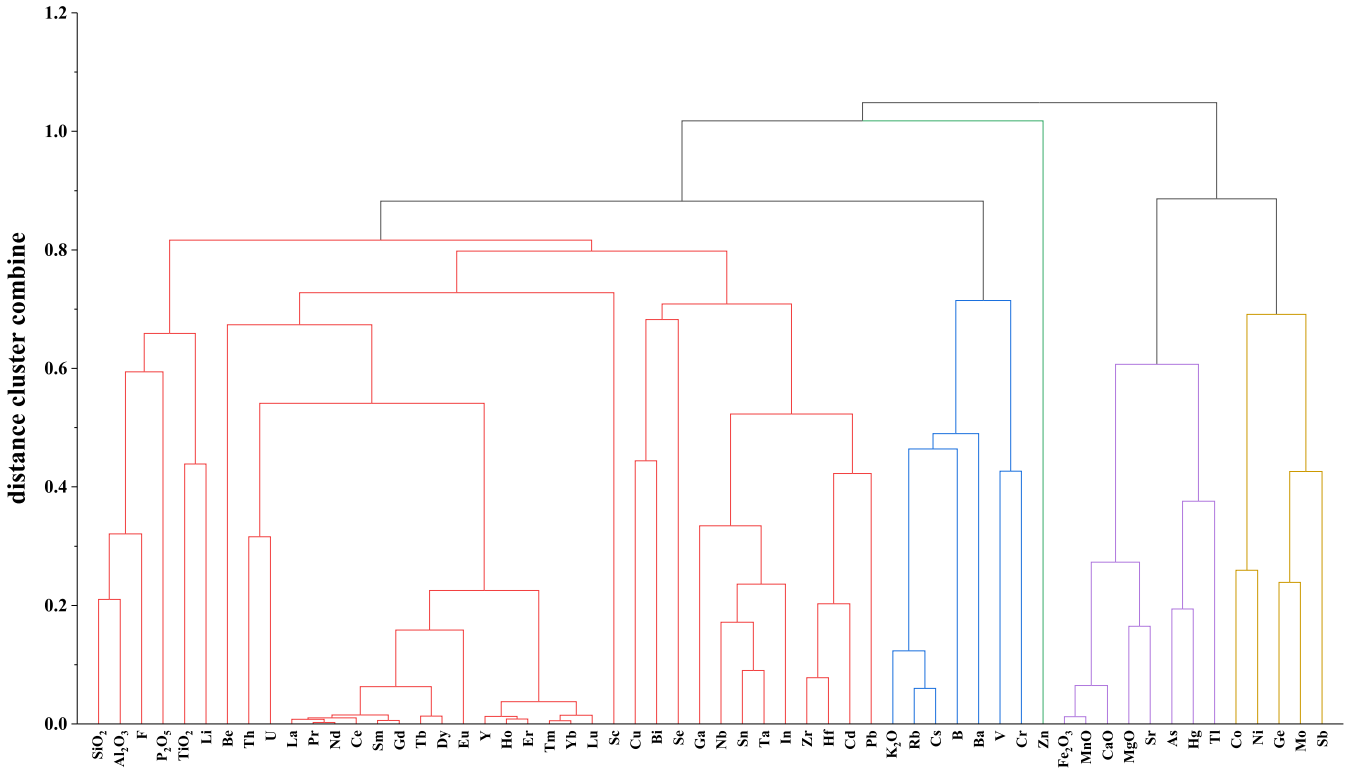

Figure 4. Average-linkage hierarchical clustering result of the Datanhao data with Pearson correlation.

correlation $\rho_{i,\,j|\boldsymbol{k}}$ can be calculated recursively with the following identity

$$\rho_{i,j|k\backslash h} = \frac{\rho_{i,j|k\backslash h} - \rho_{i,h|k\backslash h}\rho_{j,h|k\backslash h}}{\sqrt{(1-\rho^2_{i,h|k\backslash h})(1-\rho^2_{j,h|k\backslash h})}},\ h \in k \tag{1}$$

In order to test whether the partial correlation is zero or not, $\rho_{i,\,j|\boldsymbol{k}}$ needs to be transformed into a normal distribution by Fisher's z-transformation

$$Z(i,\,j|k) = \frac{1}{2}\ln\left(\frac{1+\hat{\rho}_{i,j|k}}{1-\hat{\rho}_{i,j|k}}\right) \tag{2}$$

The null hypothesis is $H_0(i,\,j|\boldsymbol{k})$:$\rho_{i,\,j|\boldsymbol{k}} = 0$, to be tested against the two-tail alternative $H_1(i,\,j|\boldsymbol{k})$:$\rho_{i,\,j|\boldsymbol{k}} \neq 0$. H_0 with significance level α will be rejected if $\sqrt{n-|k|-3}\,|Z(i,\,j|k)| > \Phi^{-1}(1-\alpha/2)$, where $\Phi(\cdot)$ denotes the cumulative distribution function of $\mathcal{N}(0,\,1)$

The only tuning parameter of the PC-skeleton algorithm (Table 1) is α, which is the significance level for testing partial correlations. In this study, the conditional independence test with a significance level of 0.05 is used to learn the skeleton of the coal elemental data. Using the width of an edge represents the minimum value of $\sqrt{n-|k|-3}\,Z(i,\,j,\,k)$ that can cause the edge, and therefore, wider edges are considered as more reliable, i.e., it represents the stronger association between two elemental vertices.

The PC-skeleton algorithm (Table 1) has been implemented in the R programming language. All of the sample data of CP2 coal from the Datanhao and Adaohai mines are used as the input as the PC-skeleton algorithm (Table 1), and the results can be obtained and discussed in the following section.

4. RESULTS AND DISCUSSION

To verify the effectiveness of the PC-skeleton algorithm (Table 1) in learning the skeleton of the Bayesian network structure of coal elemental data and analyzing the modes of occurrence of elements in coal, the whole-coal basis sample data of CP2 coal from the Datanhao and Adaohai mines are used in this study.

Based on the geochemical characteristics of elements and the investigations by Dai et al.[23] and Zhao et al.[25] using direct analytical methods (e.g., SEM-EDS, XRD), the following pairs of trace elements are geochemically similar and are expected to be adjacent in the skeleton: Sr versus Ba, Nb versus Ta, Zr versus Hf, Cd versus Zn, Hg versus As, and Rb versus Cs. In addition, the major-element oxides, including CaO, MgO, MnO, and Fe_2O_3, are expected to be adjacent. Aluminum oxide and SiO_2 are also expected to be adjacent.[1] Furthermore, edges are expected to exist between REY to reflect their associations. The Pearson correlation coefficients among the elements of Datanhao and Adaohai coals are shown in Figures 2 and 3, respectively. The larger the circles are, the stronger the correlation between the two elements is. The different colors represent different correlations; blue and red represent positive and negative correlations, respectively. Adapting the average-linkage hierarchical clustering algorithm (ALHCA)[13] as a control group, the clustering results of the Datanhao and Adaohai coals are shown in Figures 4 and 5, respectively.

4.1. Analysis of Datanhao Coal. The performance of the PC-skeleton algorithm (Table 1) is tested using 62 samples (whole-coal basis) from the Datanhao mine.

4.1.1. Major Elements. The high proportions of kaolinite, quartz, carbonate, and anatase in coal samples from the Datanhao mine are the reason for the relatively high concentrations of Al_2O_3, SiO_2, CaO, MnO, and TiO_2, as reported by Zhao et al.[25] Furthermore, aluminum oxide mainly occurs in kaolinite (the dominant clay mineral in samples from

https://doi.org/10.1021/acsomega.3c04109
ACS Omega 2023, 8, 39096−39109

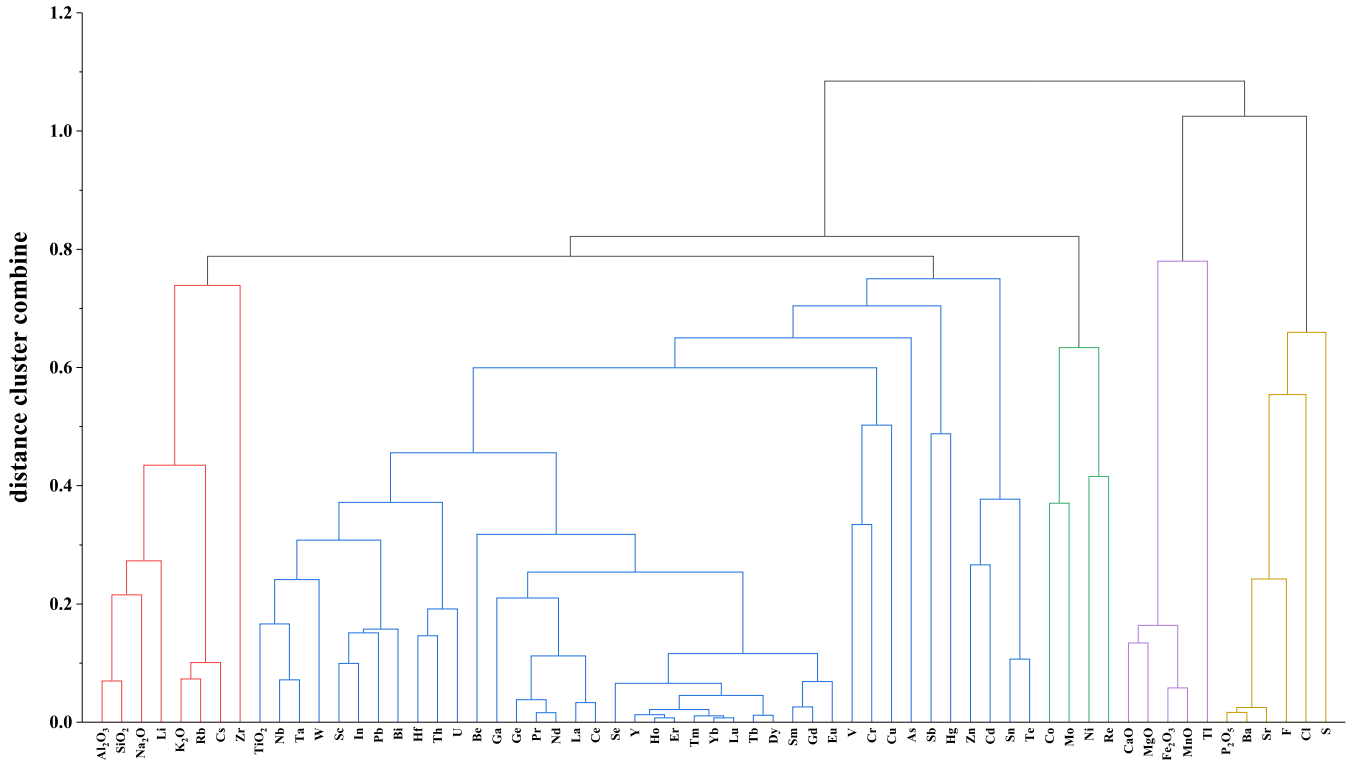

Figure 5. Average-linkage hierarchical clustering result of the Adaohai data with Pearson correlation.

the Datanhao mine), and the high concentration of SiO_2 is not only due to high proportions of clay minerals but also due to the high proportions of quartz.[25] Meanwhile, a number of studies showed that quartz and clays (particularly the prevalent kaolinite and illite) are the main hosts of Si and Al.[11,34−37]

Zhao et al.[25] have found the presence of Mn in the EDS spectra of siderite and ankerite, indicating that Mn occurs mainly in Fe-bearing minerals. In addition, Zhao et al.[38] showed that calcite, ankerite, and siderite in the Datanhao mine are well correlated, and Ca occurs mainly in calcite and ankerite. These previous studies are totally consistent with the obvious associations of Fe_2O_3, MnO, CaO, and MgO in the skeleton shown in Figure 6.

4.1.2. Strontium (Sr) and Barium (Ba). The modes of occurrence of Sr and Ba in coal have been extensively investigated,[11,37,39−41] and the results indicate that both Ba and Sr mainly have an association with carbonate and phosphate minerals. In the skeleton (Figure 6) obtained by the PC-skeleton algorithm (Table 1), the association between Sr and Ba in the Datanhao coal is obvious.

4.1.3. Cadmium (Cd) and Zinc (Zn). Note that Cd and Zn in the Datanhao coal show an obvious association in the results (Figure 6) of the PC-skeleton algorithm (Table 1), consistent with the modes of occurrence of Cd and Zn in coal and other geologic materials.[11] Zinc in coal generally occurs in sulfides such as pyrite and sphalerite, and cadmium in coal is also primarily found in sphalerite.[11,42−46]

4.1.4. Niobium (Nb), Tantalum (Ta), Zirconium (Zr), and Hafnium (Hf). Zirconium versus Hf, and Nb versus Ta are closely associated in the skeleton shown in Figure 6, respectively. Zhao et al.[25] proposed the possibility of anatase as the carrier of Zr, Hf, Nb, and Ta in the coals from the Datanhao mine, although the content of anatase in the samples is low in the samples. This can be supported by the Nb and Zr peaks found in the EDS spectra of anatase from noncoal samples.[25] Previous studies, e.g., Jiu et al.,[45] Zhang et al.,[47] and Zhang et al.,[48] further supported such association of Zr, Hf, Nb, and Ta in coal.

4.1.5. Mercury (Hg) and Arsenic (As). Zhao et al.[25] found that Hg in the Datanhao coal occurs mainly in sulfides. However, the arsenic concentration in the Datanhao coals is not available. Based on the results of SEM and EMPA, Minkin et al.[49] suggested that arsenic in coal occurs mainly in pyrite. Dai et al.,[11] Hower et al.,[50] Arbuzov et al.,[51] and Arnold[44] also concluded that arsenic in coal is mainly in pyrite and a portion is associated with organic matter. These observations are again consistent with the association of As and Hg shown in the skeleton (Figure 6).

4.1.6. Rubidium (Rb) and Cesium (Cs). For Rb and Cs in coal, Dai et al.,[11] Eminagaoglu et al.,[35] Li et al.,[52] and Ribeiro et al.[53] concluded that they are mainly associated with clay minerals. These two elements are also strongly associated with each other in the skeleton shown in Figure 6.

4.1.7. Thorium (Th) and Uranium (U). As shown in Figure 6, thorium and uranium exhibit obvious associations in the skeleton. Zhao et al.[25] noted that the main carriers of Th and U in Datanhao coal are both Ca-bearing REE-phosphate minerals, most likely to be monazite. This association can be supported by the presence of Th and U detected in monazite from the Datanhao coal by Zhao et al.[38] using SEM-EDS. Other studies also supported the association of Th and U.[1,54]

4.1.8. Cobalt (Co), Nickel (Ni), Vanadium(V), and Chromium (Cr). Coals influenced by mafic volcanic ash input or by the input of detrital materials from mafic rocks in sediment-source regions are generally rich in transition elements or metals (e.g., V, Cr, Co, and Ni).[55−61] Zhao et al.[25] calculated the Al_2O_3/TiO_2 ratios of samples from the Datanhao mine and found that a small number of samples are located in the mafic

https://doi.org/10.1021/acsomega.3c04109
ACS Omega 2023, 8, 39096−39109

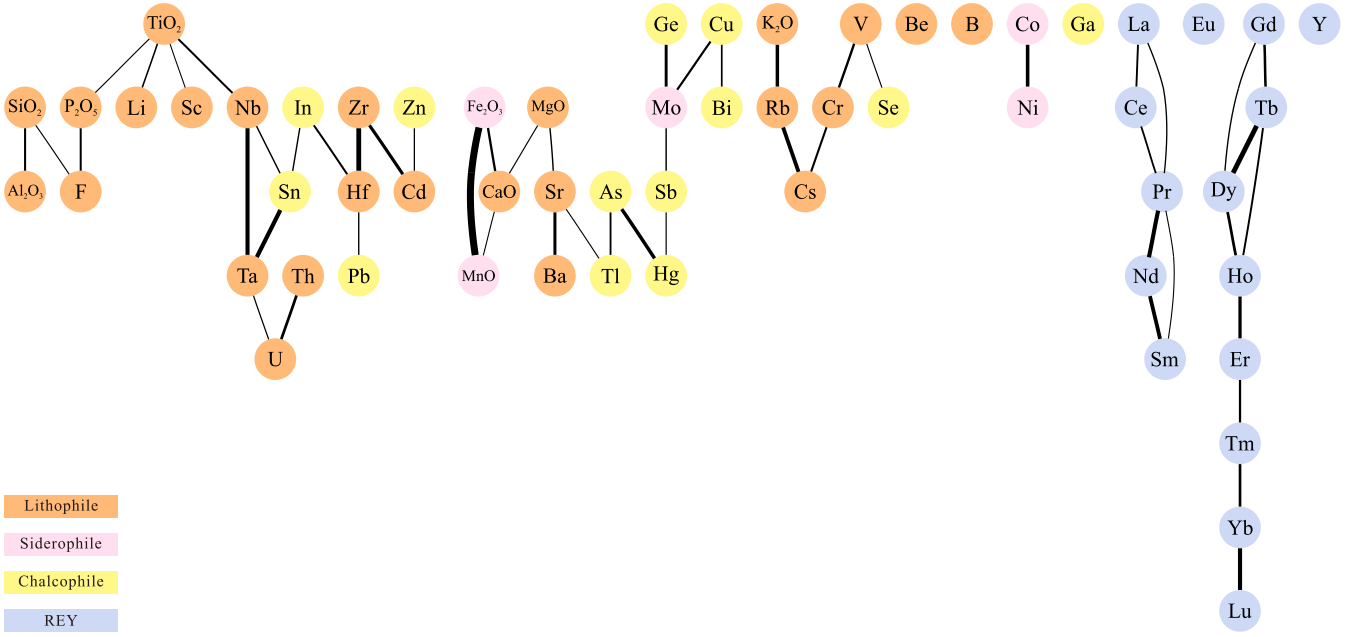

Figure 6. Skeleton of Bayesian network structure of the Datanhao coal. (The thickness of the connection indicates the strength of the association between the two elemental vertices.).

field, which likely explains the association of Co with Ni, and V with Cr in Figure 6.

4.1.9. Fluorine (F), Silicon Dioxide (SiO_2), and Phosphorus Pentoxide (P_2O_5). According to Zhao et al.,[25] fluorine of the Datanhao coal mainly occurs in kaolinite. Moreover, according to other researchers, fluorine in coal generally occurs in clay minerals, such as kaolinite, montmorillonite, illite, mica, and fluorapatite.[62−67] These observations support the association of F with SiO_2 and F with P_2O_5 of Datanhao coal in the skeleton shown in Figure 6.

4.1.10. Titanium Dioxide (TiO_2), Lithium (Li), and Scandium (Sc). Using SEM-EDS, Zhao et al.[38] indicated that some EDS-detectable Ti most likely occurring as submicron oxides are contained in kaolinite. As shown in Figure 6, titanium oxides are associated with Li, Sc, and Nb, elements commonly found in clays.

According to other studies, high concentrations of Li in Pennsylvanian coal from the Haerwusu mine in the Junger Coalfield, also located in Inner Mongolia, China, are thought to be associated with aluminosilicate minerals.[68] Wang et al.[69] used the selective leaching method to demonstrate that Li in coal is predominantly hosted in clay minerals (e.g., kaolinite and illite). Recent studies[70−72] also showed that Li in coal mainly occurs in clay minerals, consistent with the results present in this study.

For scandium, Finkelman et al.[73] found that more than half of the Sc present in bituminous and low-rank coals was associated with aluminosilicate minerals (e.g., clays) based on the selective leaching method. The concluding comments of Dai et al.[11] are that Sc in coal mainly occurs in aluminosilicates and organic matter, consistent with those reported by Chitlango et al.,[58] Hower et al.,[70] Hower et al.,[74] and Strzałkowska.[75]

4.1.11. Molybdenum (Mo), Germanium (Ge), Copper (Cu), and Antimony (Sb). Although there is no clear explanation for the associations of Mo with Ge, Mo with Sb, and Mo with Cu in the Datanhao coal, we can consider the possible associations between them from other studies. Dai et al.[11] concluded that Mo in coal is mainly associated with sulfides and organic matter; Ge in coal is almost entirely organically associated; and Sb in coal is largely associated with sulfides (mainly pyrite) and organic matter.[76−79] However, Goldschmidt[80] states that Ge is found in low-temperature sulfide minerals and Cu in coal mainly occurs in the sulfides. Therefore, this seemingly unusual association is consistent with geochemical principles.

4.1.12. REY. As observed under SEM by Zhao et al.,[25,38] the main carrier of REY is phosphate (mostly likely monazite). REY forms four subgroups in the skeleton (Figure 6) obtained by the PC-skeleton algorithm (Table 1), which obviously reflects the strong associations between the REY elements.[50,75,81,82]

4.2. Analysis of Adaohai Coal. The performance of the PC-skeleton algorithm (Table 1) is also tested using 33 coal bench samples (whole-coal basis) from the Adaohai mine.

4.2.1. Major Elements. Dai et al.[23] stated that both Al and Si are major constituents of the aluminosilicate minerals (kaolinite and illite) in the Adaohai coal. And they found carbonates (calcite, dolomite, and magnesite) in most of the studied samples, explaining the association of Fe_2O_3, MnO, CaO, and MgO in the skeleton shown in Figure 7, as these oxides are probably derived from magmatic hydrothermal fluids.[23]

4.2.2. Strontium (Sr), Barium (Ba), and Phosphorus Pentoxide (P_2O_5). Both Sr and Ba are strongly associated with P_2O_5 as shown in the skeleton (Figure 7). Dai et al.[23] indicated that Sr, Ba, and P_2O_5 occur mainly in gorceixite and fluorapatite, and this is supported by SEM-EDX data and the comparison of the XRD results with the chemical analysis. Other studies also support the association of Sr and Ba.[11,37,39−41]

4.2.3. Niobium (Nb), Tantalum (Ta), and Thorium (Th). Niobium and Ta are almost geochemically inseparable,[13,47,48] and as Dai et al.[23] suggested, thorium in the Adaohai coal mainly comes from detrital materials of the source region, which may be the same source as Nb and Ta. Therefore, it is not surprising that Th and Nb are adjacent in the skeleton (Figure 7).

4.2.4. Potassium Oxide (K_2O), Rubidium (Rb), and Cesium (Cs). Both Rb and Cs are strongly associated with K_2O (Figure 7) in the results of the PC-skeleton algorithm (Table 1). Dai et al.[23] noted that Rb, Cs, and K_2O in the Adaohai coal have high aluminosilicate affinity, and are probably associated with

https://doi.org/10.1021/acsomega.3c04109
ACS Omega 2023, 8, 39096−39109

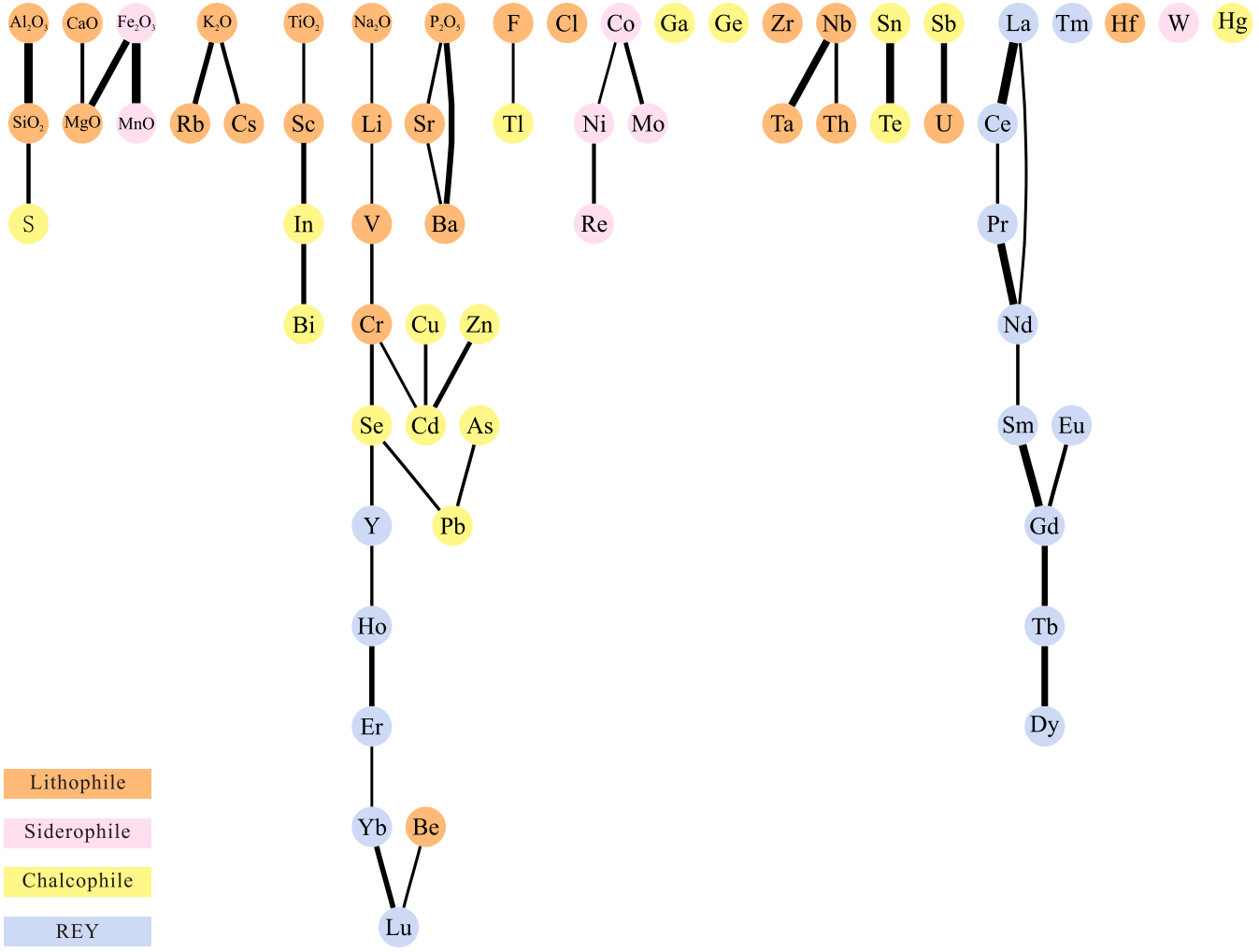

Figure 7. Skeleton of Bayesian network structure of the Adaohai coal. (The thickness of connection indicates the strength of the association between the two elemental vertices.).

diaspore and clay minerals. Previous studies[35,52,53] also supported the association of Rb and Cs, consistent with the results presented in this paper.

4.2.5. Titanium Dioxide (TiO_2), Scandium (Sc), Indium (In), and Bismuth (Bi). These elements are universally found in heavy mineral assemblages, where TiO_2 and Sc are lipophilic elements present in aluminosilicates.[23,58,70,74,75] An interesting result is that In and Bi show obvious associations in the skeleton (Figure 7). Dai et al.[11] concluded that although various modes of occurrence of In and Bi in coal have been reported,[83−87] their degree of certainty is not high. Goldschmidt[80] mentions that In, though primarily a chacophile/siderophile element, is associated with tin detrital minerals and that Bi is found with Nb and Ta in granites. Thus, the association of these elements may indicate a common detrital source.

4.2.6. Vanadium(V), Chromium (Cr), Cadmium (Cd), Zinc (Zn), Tin (Sn), and Tellurium (Te). Dai et al.[23] suggested that the elements in this group from the Adaohai coal are probably associated with unidentified traces of sulfide minerals.

As shown in Figure 7, vanadium, Cr, Cd, and Zn are associated with the skeleton. From the results of previously reported studies, we found some associations of Cr with sulfide minerals. Huggins et al.[88] found that a small amount of Cr in coal occurs in chromian magnetite and sulfides. Ruppert et al.[89] investigated the modes of occurrence of Cr in Pliocene lignite from the Kosovo Basin, southern Serbia, and found that Cr is associated, to a lesser extent, with authigenic minerals (e.g., sulfides and Ni−Fe sulfates). In addition, Dai et al.[11] concluded that Cd and Zn in coal mainly occur in sphalerite. Zhuang et al.[90] discovered a sulfide association for Zn and Cd by investigating coal samples from the Chongqing coal district, Southwestern China. Tian et al.[91] found that Zn and Cd are strongly associated with pyrite by a combination of float-sink and low-temperature ashing. Recent studies, e.g., Arnold et al.,[44] Jiu et al.,[45] and Li et al.,[46] further supported such association of Cd and Zn in coal.

Tellurium and Sn show an obvious association in the skeleton (Figure 7). Although various forms of Sn in coal have been reported, its common mode of occurrence has not been clearly identified.[11] Vassilev et al.[92] found Sn in sulfide (pyrite and marcasite) and carbonate (rhodochrosite, dolomite, and ankerite) impurities of Bobov Dol coals in Bulgaria. Tian et al.[91] combined low-temperature ashing and float-sink technique to demonstrate a clear association of Sn with pyrite in coal. Bullock et al.[93] found Te enrichment at the pyrite rim of the coal using LA-ICP-MS techniques. In addition, Bullock et al.[94] indicated that the average concentration of Te is associated with early syngenetic and later cleat-filling pyrite by investigating British Carboniferous coals.

4.2.7. Cobalt (Co), Molybdenum (Mo), Nickel (Ni), and Rhenium (Re). As shown in Figure 7, Co, Mo, Ni, and Re are

https://doi.org/10.1021/acsomega.3c04109
ACS Omega 2023, 8, 39096−39109

closely associated, which is to be expected for these siderophile elements.[80] This relationship is interesting as there is very little information on the modes of occurrence of Re.[95−97] Dai et al.[11] pointed out that the certainty of the modes of occurrence of Re in coal is low because none has been verified, and the association of Re with Co, Mo, and Ni in the Adaohai coal implies likely sulfide association.

4.2.8. Uranium (U) and Antimony (Sb). Although U and Sb in Adaohai coal show an obvious association in the skeleton shown in Figure 7, no clear geochemical explanation has been found. As concluded by Dai et al.,[11] Sb in coal is mainly associated with sulfide (mainly pyrite) and organic matter, and U in coal generally exhibits organic associations.

4.2.9. Zirconium (Zr) and Hafnium (Hf). According to Dai et al.,[23] if Zr partially occurs in clay minerals, it may explain the unusual lack of the association of Zr with Hf in the skeleton (Figure 7) obtained by the PC-skeleton algorithm (Table 1).

4.2.10. REY. REY forms three subgroups in the skeleton (Figure 7) obtained by the PC-skeleton algorithm (Table 1), in which Tm is not adjacent to any other elements. The other two groups contain the remaining elements in REY, where yttrium is adjacent to Se and Lu is adjacent to Be.

4.3. Performance Evaluation. *4.3.1. Datanhao Coal.* Strontium versus Ba, Cd versus Zn, Nb versus Ta, Zr versus Hf, Hg versus As, and Rb versus Cs are adjacent in the skeleton (Figure 6) obtained by the PC-skeleton algorithm (Table 1), respectively. Except for Cd versus Zn, all of the above groups have distinct wider edges representing the more reliable association relationships of elements. Zirconium versus Hf, Hg versus As, and Rb versus Cs are clustered together at the early clustering stages (Figure 4) by the ALHCA, respectively. As shown in Figure 2A, r_{Sr-Ba} = 0.72 (r, Pearson correlation coefficient), r_{Cd-Zn} = 0.40, r_{Nb-Ta} = 0.91, r_{Zr-Hf} = 0.92, r_{As-Hg} = 0.81, and r_{Cs-Rb} = 0.94.

As shown in Figure 6, Al_2O_3 and SiO_2 are adjacent to each other in the skeleton. Oxides (e.g., CaO, MgO, MnO, and Fe_2O_3) are also connected, with the widest edge between MnO and Fe_2O_3. In the results from ALHCA, Al_2O_3 and SiO_2 are clustered together at the early clustering stages (Figure 4). Calcium oxide, MnO, and Fe_2O_3 are clustered together at the early clustering stages, but MgO is clustered together with Sr at the early clustering stages rather than being clustered together with the cluster formed by CaO, MnO, and Fe_2O_3 (Figure 4). The correlation coefficient of Al_2O_3 and SiO_2 is 0.79 (Figure 2B). Calcium oxide, MgO, MnO, and Fe_2O_3 have correlation coefficients greater than 0.71 with each other (Figure 2B).

The light REE (La, Ce, Pr, Nd, and Sm) and heavy REE (Ho, Er, Tm, Yb, and Lu) are closely associated in the skeleton (Figure 6), respectively. Except for Eu and Y, the middle REE (Gd, Tb, and Dy) is closely associated. In the result of ALHCA, REY clusters together at the early clustering stages (Figure 4), which is consistent with the geochemical characteristics of REY. Except for Eu and Lu (r_{Eu-Lu} = 0.49), the correlation coefficients between REY all exceed 0.52 and the majority of them exceed 0.70 (Figure 2C).

4.3.2. Adaohai Coal. In the skeleton (Figure 7) obtained by the PC-skeleton algorithm (Table 1), Cd with Zn, Nb with Ta, and Sr with Ba are adjacent to each other, respectively. And Cd with Zn, Nb with Ta have distinct wider edges. Cadmium with Zn and Nb with Ta are clustered together at the early clustering stages (Figure 5) by the ALHCA, respectively. As shown in Figure 3A, r_{Cd-Zn} = 0.73, r_{Nb-Ta} = 0.93, and r_{Sr-Ba} = 0.98.

As shown in Figure 7, Al_2O_3 and SiO_2 are adjacent and the edges connecting them are obviously wide. Calcium oxide, MgO, MnO, and Fe_2O_3 which mainly occur in the carbonate minerals,[23] are connected in the skeleton and there are also distinctly wide edges between them (Figure 7). In the result of the ALHCA (Figure 5), Al_2O_3 and SiO_2 are clustered together at the early clustering stages; calcium oxide, MgO, MnO, and Fe_2O_3 cluster together at the early clustering stages (Figure 5). The correlation coefficient of Al_2O_3 and SiO_2 is 0.93 (Figure 3B). Calcium oxide, MgO, MnO, and Fe_2O_3 have correlation coefficients higher than 0.78 with each other (Figure 3B).

Light REE (La, Ce, Pr, Nd, and Sm) and middle REE (Eu, Gd, Tb, and Dy) are closely associated in the skeleton (Figure 7). Yttrium, heavy REE (Ho, Er, Yb, and Lu), Y, Be, and Se are closely associated in the skeleton, except for Tm (Figure 7). In the result of the ALHCA, REY elements are obviously clustered together overall, but Ga and Ge are also clustered together with them at an early clustering stage (Figure 5). All correlation coefficients between REY exceed 0.59, and the majority of them exceeds 0.70 (Figure 3C).

In terms of sulfur, both the Datanhao and Adaohai coals are low-sulfur coals.[23,25] Sulfur in low-sulfur coal, as reported by Chou[98] and Dai et al.,[99] was derived primarily from parent plant materials, and in most cases, low-sulfur coals formed in nonmarine influenced environments.[98−101] Sulfur in such low-sulfur coals has a very little effect on both abundance and modes of occurrence of other elements in coal,[102−104] different from that in high-sulfur coals (total sulfur higher than 3%).[105−107] Therefore, the impact of sulfur on the modes of occurrence of trace elements in Datanhao and Adaohai coals is not significant.

5. CONCLUSIONS

In this study, we conducted extensive experiments by applying the PC-skeleton algorithm (Table 1) to samples collected from the Datanhao and Adaohai mines to learn the skeleton of the coal elemental data (i.e., the dependence relationships between elements). Experimental results show that the PC-skeleton algorithm (Table 1) is more effective in inferring modes of occurrence of elements in coal than the average-linkage hierarchical clustering algorithm. Based on the comprehensive studies, the main conclusions are drawn as follows:

(1) The ALHCA fails to accurately explain the association between Sr and Ba in the Datanhao coal (Figure 4). However, the PC-skeleton algorithm (Table 1) clearly reveals the association between Sr and Ba in the Datanhao coal (Figure 6). This result is aligned with the geochemical nature and Ba and Sr are predominantly associated with carbonate and phosphate minerals.

(2) In the skeleton obtained by the PC-skeleton algorithm (Figure 6), the association between Cd and Zn in the Datanhao coal is obvious, which is consistent with the geochemical nature. Zinc in coal is typically found in sulfides like pyrite and sphalerite, and cadmium primarily occurs in sphalerite as well. However, the association between Cd and Zn is noticeably absent in the results of ALHCA (Figure 4).

(3) Thorium in the Adaohai coal mainly comes from detrital materials of the source region, which is probably the same source as Nb and Ta. It is reasonable that thorium and niobium show an association in the skeleton (Figure 7), but thorium is not closely associated with Nb or Ta in the result of ALHCA (Figure 5).

https://doi.org/10.1021/acsomega.3c04109
ACS Omega 2023, 8, 39096−39109

The PC-skeleton algorithm (Table 1) always clusters each element during iteration; thus, each element represented by a vertex does not lose its geochemical meaning during the clustering process, unlike the case of hierarchical clustering. Consequently, the PC-skeleton algorithm (Table 1) is more accurate in analyzing the modes of occurrence of elements in coal. Therefore, it can provide new insight into inferring the modes of occurrence of elements in coal.

While the results are totally consistent with established geochemical principles and published research on the modes of occurrence of elements in coal, we acknowledge that there are still a few anomalies. A few unexpected relationships e.g., the relationship of Tl and F (Figure 7), the relationship of U and Sb (Section 4.2.8), and the lack of relationship of Zr and Hf (Section 4.2.9) exist. These cases present opportunities for additional research to clarify the modes of occurrence of elements in coal.

■ ASSOCIATED CONTENT

Data Availability Statement

The data underlying this study are openly available at 10.17632/74pcrhknp7.1.

■ AUTHOR INFORMATION

Corresponding Author

Na Xu − *College of Geoscience and Survey Engineering, China University of Mining and Technology (Beijing), Beijing 100083, China;* orcid.org/0000-0002-1406-9098; Email: xuna1011@gmail.com

Authors

Qiang Li − *College of Geoscience and Survey Engineering, China University of Mining and Technology (Beijing), Beijing 100083, China*

Wei Zhu − *College of Geoscience and Survey Engineering, China University of Mining and Technology (Beijing), Beijing 100083, China*

Qing Li − *Department of Computing, Hong Kong Polytechnic University, Hong Kong, China*

Robert B. Finkelman − *College of Geoscience and Survey Engineering, China University of Mining and Technology (Beijing), Beijing 100083, China; University of Texas at Dallas, Richardson, Texas 75080, United States*

Mark A. Engle − *Department of Earth, Environmental and Resource Sciences, University of Texas at El Paso, El Paso, Texas 79968, United States*

Ru Wang − *College of Geoscience and Survey Engineering, China University of Mining and Technology (Beijing), Beijing 100083, China*

Zhiwei Wang − *College of Geoscience and Survey Engineering, China University of Mining and Technology (Beijing), Beijing 100083, China*

Complete contact information is available at: https://pubs.acs.org/10.1021/acsomega.3c04109

Author Contributions

The manuscript was written through contributions of all authors. All authors have given approval to the final version of the manuscript.

Notes

The authors declare no competing financial interest.

■ ACKNOWLEDGMENTS

This research was funded by the National Key Research and Development Program of China (no. 2021YFC2902005).

■ REFERENCES

(1) Dai, S.; Finkelman, R. B.; Hower, J. C.; French, D.; Graham, I. T.; Zhao, L. *Inorganic Geochemistry of Coal*; Elsevier, 2023.

(2) Ward, C. R. Analysis and Significance of Mineral Matter in Coal Seams. *Int. J. Coal Geol.* **2002**, *50* (1−4), 135−168.

(3) Ward, C. R. Analysis, Origin and Significance of Mineral Matter in Coal: An Updated Review. *Int. J. Coal Geol.* **2016**, *165*, 1−27.

(4) Dai, S.; Finkelman, R. B. Coal as a Promising Source of Critical Elements: Progress and Future Prospects. *Int. J. Coal Geol.* **2018**, *186*, 155−164.

(5) Laudal, D. A.; Benson, S. A.; Addleman, R. S.; Palo, D. Leaching Behavior of Rare Earth Elements in Fort Union Lignite Coals of North America. *Int. J. Coal Geol.* **2018**, *191*, 112−124.

(6) Montross, S. N.; Verba, C. A.; Chan, H. L.; Lopano, C. Advanced Characterization of Rare Earth Element Minerals in Coal Utilization Byproducts Using Multimodal Image Analysis. *Int. J. Coal Geol.* **2018**, *195*, 362−372.

(7) Finkelman, R. B.; Dai, S.; French, D. The Importance of Minerals in Coal as the Hosts of Chemical Elements: A Review. *Int. J. Coal Geol.* **2019**, *212*, No. 103251.

(8) Erickson, T. A.; Allan, S. E.; McCollor, D. P.; Hurley, J. P.; Srinivasachar, S.; Kang, S. G.; Baker, J. E.; Morgan, M. E.; Johnson, S. A.; Borio, R. Modelling of Fouling and Slagging in Coal-Fired Utility Boilers. *Fuel Process. Technol.* **1995**, *44* (1), 155−171.

(9) Zhao, L.; Dai, S.; Finkelman, R. B.; French, D.; Graham, I. T.; Yang, Y.; Li, J.; Yang, P. Leaching Behavior of Trace Elements from Fly Ashes of Five Chinese Coal Power Plants. *Int. J. Coal Geol.* **2020**, *219*, No. 103381.

(10) Dai, S.; Ren, D.; Chou, C.-L.; Finkelman, R. B.; Seredin, V. V.; Zhou, Y. Geochemistry of Trace Elements in Chinese Coals: A Review of Abundances, Genetic Types, Impacts on Human Health, and Industrial Utilization. *Int. J. Coal Geol.* **2012**, *94*, 3−21.

(11) Dai, S.; Finkelman, R. B.; French, D.; Hower, J. C.; Graham, I. T.; Zhao, F. Modes of Occurrence of Elements in Coal: A Critical Evaluation. *Earth-Sci. Rev.* **2021**, *222*, No. 103815.

(12) Xu, R.; Wunsch, D. Survey of Clustering Algorithms. *IEEE Trans. Neural Netw.* **2005**, *16* (3), 645−678.

(13) Xu, N.; Finkelman, R. B.; Dai, S.; Xu, C.; Peng, M. Average Linkage Hierarchical Clustering Algorithm for Determining the Relationships between Elements in Coal. *ACS Omega* **2021**, *6* (9), 6206−6217.

(14) Xu, N.; Xu, C.; Finkelman, R. B.; Engle, M. A.; Li, Q.; Peng, M.; He, L.; Huang, B.; Yang, Y. Coal Elemental (Compositional) Data Analysis with Hierarchical Clustering Algorithms. *Int. J. Coal Geol.* **2022**, *249*, No. 103892.

(15) Chen, R. Causal Network Inference for Neural Ensemble Activity. *Neuroinform.* **2021**, *19* (3), 515−527.

(16) Gopnik, A.; Glymour, C.; Sobel, D. M.; Schulz, L. E.; Kushnir, T.; Danks, D. A Theory of Causal Learning in Children: Causal Maps and Bayes Nets. *Psychol. Rev.* **2004**, *111* (1), 3−32.

(17) Jayech, K.; Mahjoub, M. A.; Ghanmi, N. In *Application of Bayesian Networks for Pattern Recognition: Character Recognition Case*, 2012 6th International Conference on Sciences of Electronics, Technologies of Information and Telecommunications (SETIT), 2012; pp 748−757.

(18) Lo, C. H.; Wong, Y. K.; Rad, A. B. Bond Graph Based Bayesian Network for Fault Diagnosis. *Appl. Soft Comput.* **2011**, *11* (1), 1208−1212.

(19) Luo, G.; Zhao, B.; Du, S. Causal Inference and Bayesian Network Structure Learning from Nominal Data. *Appl. Intell.* **2019**, *49* (1), 253−264.

(20) Wang, Q.; Gao, X.; Chen, D. In *Pattern Recognition for Ship Based on Bayesian Networks*, Fourth International Conference on Fuzzy Systems and Knowledge Discovery (FSKD 2007), 2007; pp 684−688.

(21) Zhao, Y.; Chen, Y.; Tu, K.; Tian, J. Learning Bayesian Network Structures under Incremental Construction Curricula. *Neurocomputing* **2017**, *258*, 30−40.
(22) Li, H.; Guo, H. A Hybrid Structure Learning Algorithm for Bayesian Network Using Experts' Knowledge. *Entropy* **2018**, *20* (8), 620.
(23) Dai, S.; Zou, J.; Jiang, Y.; Ward, C. R.; Wang, X.; Li, T.; Xue, W.; Liu, S.; Tian, H.; Sun, X.; Zhou, D. Mineralogical and Geochemical Compositions of the Pennsylvanian Coal in the Adaohai Mine, Daqingshan Coalfield, Inner Mongolia, China: Modes of Occurrence and Origin of Diaspore, Gorceixite, and Ammonian Illite. *Int. J. Coal Geol.* **2012**, *94*, 250−270.
(24) Dai, S.; Li, T.; Jiang, Y.; Ward, C. R.; Hower, J. C.; Sun, J.; Liu, J.; Song, H.; Wei, J.; Li, Q.; Xie, P.; Huang, Q. Mineralogical and Geochemical Compositions of the Pennsylvanian Coal in the Hailiushu Mine, Daqingshan Coalfield, Inner Mongolia, China: Implications of Sediment-Source Region and Acid Hydrothermal Solutions. *Int. J. Coal Geol.* **2015**, *137*, 92−110.
(25) Zhao, L.; Dai, S.; Nechaev, V. P.; Nechaeva, E. V.; Graham, I. T.; French, D.; Sun, J. Enrichment of Critical Elements (Nb-Ta-Zr-Hf-REE) within Coal and Host Rocks from the Datanhao Mine, Daqingshan Coalfield, Northern China. *Ore Geol. Rev.* **2019**, *111*, No. 102951.
(26) Ketris, M. P.; Yudovich, Ya. E. Estimations of Clarkes for Carbonaceous Biolithes: World Averages for Trace Element Contents in Black Shales and Coals. *Int. J. Coal Geol.* **2009**, *78* (2), 135−148.
(27) Pearl, J. *Probabilistic Reasoning in Intelligent Systems: Networks of Plausible Inference*; Morgan Kaufmann: San Francisco, 1988.
(28) Kalisch, M.; Buehlmann, P. Estimating High-Dimensional Directed Acyclic Graphs with the PC-Algorithm. *J. Mach. Learn. Res.* **2007**, *8*, 613−636.
(29) Chickering, D. M. Optimal Structure Identification with Greedy Search. *J. Mach. Learn. Res.* **2002**, *3* (Nov), 507−554.
(30) Ramsey, J.; Glymour, M.; Sanchez-Romero, R.; Glymour, C. A Million Variables and More: The Fast Greedy Equivalence Search Algorithm for Learning High-Dimensional Graphical Causal Models, with an Application to Functional Magnetic Resonance Images. *Int. J. Data Sci. Anal.* **2017**, *3* (2), 121−129.
(31) Aragam, B.; Zhou, Q. Concave Penalized Estimation of Sparse Gaussian Bayesian Networks. *J. Mach. Learn. Res.* **2015**, *16*, 2273−2328.
(32) Colombo, D.; Maathuis, M. H. Order-Independent Constraint-Based Causal Structure Learning. *J. Mach. Learn. Res.* **2014**, *15* (1), 3741−3782.
(33) Lauritzen, S. L. *Graphical Models*; Clarendon Press, 1996.
(34) Di, S.; Dai, S.; Nechaev, V. P.; Zhang, S.; French, D.; Graham, I. T.; Spiro, B.; Finkelman, R. B.; Hou, Y.; Wang, Y.; Zhang, R. Granite-Bauxite Provenance of Abnormally Enriched Boehmite and Critical Elements (Nb, Ta, Zr, Hf and Ga) in Coals from the Eastern Surface Mine, Ningwu Coalfield, Shanxi Province, China. *J. Geochem. Explor.* **2022**, *239*, No. 107016.
(35) Eminagaoglu, M.; Oskay, R. G.; Karayigit, A. I. Evaluation of Elemental Affinities in Coal Using Agglomerative Hierarchical Clustering Algorithm: A Case Study in a Thick and Mineable Coal Seam (KM2) from Soma Basin (W. Turkey). *Int. J. Coal Geol.* **2022**, *259*, No. 104045.
(36) Harrar, H.; Eterigho-Ikelegbe, O.; Modiga, A.; Bada, S. Mineralogy and Distribution of Rare Earth Elements in the Waterberg Coalfield High Ash Coals. *Miner. Eng.* **2022**, *183*, No. 107611.
(37) Hou, Y.; Dai, S.; Nechaev, V. P.; Finkelman, R. B.; Wang, H.; Zhang, S.; Di, S. Mineral Matter in the Pennsylvanian Coal from the Yangquan Mining District, Northeastern Qinshui Basin, China: Enrichment of Critical Elements and a Se-Mo-Pb-Hg Assemblage. *Int. J. Coal Geol.* **2023**, *266*, No. 104178.
(38) Zhao, L.; Sun, J.; Guo, W.; Wang, P.; Ji, D. Mineralogy of the Pennsylvanian Coal Seam in the Datanhao Mine, Daqingshan Coalfield, Inner Mongolia, China: Genetic Implications for Mineral Matter in Coal Deposited in an Intermontane Basin. *Int. J. Coal Geol.* **2016**, *167*, 201−214.
(39) Hou, Y.; Liu, D.; Zhao, F.; Zhang, S.; Zhang, Q.; Emmanuel, N. N.; Zhong, L. Mineralogical and Geochemical Characteristics of Coal from the Southeastern Qinshui Basin: Implications for the Enrichment and Economic Value of Li and REY. *Int. J. Coal Geol.* **2022**, *264*, No. 104136.
(40) Karayigit, A. I.; Azeri, N.; Oskay, R. G.; Hower, J. C. Zeolite and Associated Mineral Occurrences in High-Sulphur Coals from the Middle Miocene Upper Coal Seam from Underground Mines in the Çayirhan Coalfield, (Beypazarı, Central Turkey). *Int. J. Coal Geol.* **2022**, *256*, No. 104010.
(41) Sanders, M. M.; Rimmer, S. M.; Rowe, H. D. Carbon Isotopic Composition and Organic Petrography of Thermally Metamorphosed Antarctic Coal: Implications for Evaluation of Δ13Corg Excursions in Paleo-Atmospheric Reconstruction. *Int. J. Coal Geol.* **2023**, *267*, No. 104182.
(42) Diehl, S. F.; Goldhaber, M. B.; Hatch, J. R. Modes of Occurrence of Mercury and Other Trace Elements in Coals from the Warrior Field, Black Warrior Basin, Northwestern Alabama. *Int. J. Coal Geol.* **2004**, *59* (3), 193−208.
(43) Hower, J. C.; Campbell, J. L. Iain.; Teesdale, W. J.; Nejedly, Z.; Robertson, J. D. Scanning Proton Microprobe Analysis of Mercury and Other Trace Elements in Fe-Sulfides from a Kentucky Coal. *Int. J. Coal Geol.* **2008**, *75* (2), 88−92.
(44) Arnold, B. J. A Review of Element Partitioning in Coal Preparation. *Int. J. Coal Geol.* **2023**, *274*, No. 104296.
(45) Jiu, B.; Huang, W.; Spiro, B.; Hao, R.; Mu, N.; Wen, L.; Hao, H. Distribution of Li, Ga, Nb, and REEs in Coal as Determined by LA-ICP-MS Imaging: A Case Study from Jungar Coalfield, Ordos Basin, China. *Int. J. Coal Geol.* **2023**, *267*, No. 104184.
(46) Li, X.; Sun, G.; Wu, Y.; Zhou, M.; Li, Z.; Bi, X.; Huang, J.-H.; Feng, X. Origin and Geochemical Significance of Antimony in Chinese Coal. *Int. J. Coal Geol.* **2023**, *265*, No. 104165.
(47) Zhang, S.; Xiu, W.; Sun, B.; Liu, Q. Provenance of Multi-Stage Volcanic Ash Recorded in the Late Carboniferous Coal in the Jungar Coalfield, North China, and Their Contribution to the Enrichment of Critical Metals in the Coal. *Int. J. Coal Geol.* **2023**, *273*, No. 104265.
(48) Zhang, Z.; Lv, D.; Hower, J. C.; Wang, L.; Shen, Y.; Zhang, A.; Xu, J.; Gao, J. Geochronology, Mineralogy, and Geochemistry of Tonsteins from the Pennsylvanian Taiyuan Formation of the Jungar Coalfield, Ordos Basin, North China. *Int. J. Coal Geol.* **2023**, *267*, No. 104183.
(49) Minkin, J. A.; Finkelman, R. B.; Thompson, C. L.; Chao, E. C. T.; Ruppert, L. F.; Blank, H.; Cecil, C. B. Microcharacterization of Arsenic-And Selenium-Bearing Pyrite In Upper Freeport Coal, Indiana County, Pennsylvania. *Scanning Electron Microsc.* **1984**, No. Issue 4, 1515−1529.
(50) Hower, J. C.; Eble, C. F.; Hopps, S. D.; Morgan, T. D. Aspects of Rare Earth Element Geochemistry of the Pond Creek Coalbed, Pike County, Kentucky. *Int. J. Coal Geol.* **2022**, *261*, No. 104082.
(51) Arbuzov, S. I.; Chekryzhov, I. Yu.; Verkhoturov, A. A.; Spears, D. A.; Melkiy, V. A.; Zarubina, N. V.; Blokhin, M. G. Geochemistry and Rare-Metal Potential of Coals of the Sakhalin Coal Basin, Sakhalin Island, Russia. *Int. J. Coal Geol.* **2023**, *268*, No. 104197.
(52) Li, J.; Wang, Y.; Nguyen, X.; Zhuang, X.; Li, J.; Querol, X.; Li, B.; Moreno, N.; Hoang, V.; Cordoba, P.; Do, V. First Insights into Mineralogy, Geochemistry, and Isotopic Signatures of the Upper Triassic High-sulfur Coals from the Thai Nguyen Coal Field, NE Vietnam. *Int. J. Coal Geol.* **2022**, *261*, No. 104097.
(53) Ribeiro, J.; Suárez-Ruiz, I.; Flores, D. Coal Related Fires in Portugal: New Occurrences and New Insights on the Characterization of Thermally Affected and Non-Affected Coal Waste Piles. *Int. J. Coal Geol.* **2022**, *252*, No. 103941.
(54) Machovič, V.; Havelcová, M.; Lapčák, L.; Mizera, J.; Sýkorová, I. Chemical Character and Structure of Uraniferous Bitumens (Vrchlabí, Czech Republic). *Int. J. Coal Geol.* **2022**, *264*, No. 104137.
(55) Dai, S.; Luo, Y.; Seredin, V. V.; Ward, C. R.; Hower, J. C.; Zhao, L.; Liu, S.; Zhao, C.; Tian, H.; Zou, J. Revisiting the Late Permian Coal from the Huayingshan, Sichuan, Southwestern China: Enrichment and Occurrence Modes of Minerals and Trace Elements. *Int. J. Coal Geol.* **2014**, *122*, 110−128.

https://doi.org/10.1021/acsomega.3c04109
ACS Omega 2023, 8, 39096−39109

(56) Wang, P.; Yan, X.; Guo, W.; Zhang, S.; Wang, Z.; Xu, Y.; Wang, L. Geochemistry of Trace Elements in Coals from the Yueliangtian Mine, Western Guizhou, China: Abundances, Modes of Occurrence, and Potential Industrial Utilization. *Energy Fuels* **2016**, *30* (12), 10268−10281.
(57) Zhao, L.; Ward, C. R.; French, D.; Graham, I. T. Major and Trace Element Geochemistry of Coals and Intra-Seam Claystones from the Songzao Coalfield, SW China. *Minerals* **2015**, *5* (4), 870−893.
(58) Chitlango, F. Z.; Wagner, N. J.; Moroeng, O. M. Characterization and Pre-Concentration of Rare Earth Elements in Density Fractionated Samples from the Waterberg Coalfield, South Africa. *Int. J. Coal Geol.* **2023**, *275*, No. 104299.
(59) Dai, S.; Li, T.; Seredin, V. V.; Ward, C. R.; Hower, J. C.; Zhou, Y.; Zhang, M.; Song, X.; Song, W.; Zhao, C. Origin of Minerals and Elements in the Late Permian Coals, Tonsteins, and Host Rocks of the Xinde Mine, Xuanwei, Eastern Yunnan, China. *Int. J. Coal Geol.* **2014**, *121*, 53−78.
(60) Patria, A. A.; Anggara, F. Petrological, Mineralogical, and Geochemical Compositions of Coal in the Ombilin Basin, West Sumatra, Indonesia. *Int. J. Coal Geol.* **2022**, *262*, No. 104099.
(61) Zhou, M.; Dai, S.; Wang, X.; Zhao, L.; Nechaev, V. P.; French, D.; Graham, I. T.; Zheng, J.; Wang, Y.; Dong, M. Critical Element (Nb-Ta-Zr-Hf-REE-Ga-Th-U) Mineralization in Late Triassic Coals from the Gaosheng Mine, Sichuan Basin, Southwestern China: Coupled Effects of Products of Sediment-Source-Region Erosion and Acidic Water Infiltration. *Int. J. Coal Geol.* **2022**, *262*, No. 104101.
(62) Beising, R.; Kirsch, H. Behavior of the Trace Element Fluorine during the Combustion of Fossil Fuels. *VGB Kraftswerkstech* **1974**, *54* (4), 268−286.
(63) Thomas, J., Jr.; Glass, H. D.; White, W. A.; Trandel, R. M. Fluoride Content of Clay Minerals and Argillaceous Earth Materials. *Clays Clay Miner.* **1977**, *25* (4), 278−284.
(64) Greta, E.; Dai, S.; Li, X. Fluorine in Bulgarian Coals. *Int. J. Coal Geol.* **2013**, *105*, 16−23.
(65) Dai, S.; Hower, J. C.; Ward, C. R.; Guo, W.; Song, H.; O'Keefe, J. M. K.; Xie, P.; Hood, M. M.; Yan, X. Elements and Phosphorus Minerals in the Middle Jurassic Inertinite-Rich Coals of the Muli Coalfield on the Tibetan Plateau. *Int. J. Coal Geol.* **2015**, *144−145*, 23−47.
(66) Guohua, L.; Qiyan, F.; Xiaoli, D.; Yahong, C.; Wenbo, L.; Hui, W.; Bo, G.; Lai, Z.; Xin, W. Geochemical Characteristics of Fluorine in Coal within Xiangning Mining Area, China, and Associated Mitigation Countermeasures. *Energy Explor. Exploit.* **2019**, *37* (6), 1737−1751.
(67) Davis, B. A.; Rodrigues, S.; Esterle, J. S.; Nguyen, A. D.; Duxbury, A. J.; Golding, S. D. Geochemistry of Apatite in Late Permian Coals, Bowen Basin, Australia. *Int. J. Coal Geol.* **2021**, *237*, No. 103708.
(68) Dai, S.; Li, D.; Chou, C.-L.; Zhao, L.; Zhang, Y.; Ren, D.; Ma, Y.; Sun, Y. Mineralogy and Geochemistry of Boehmite-Rich Coals: New Insights from the Haerwusu Surface Mine, Jungar Coalfield, Inner Mongolia, China. *Int. J. Coal Geol.* **2008**, *74* (3), 185−202.
(69) Wang, X.; Wang, X.; Pan, Z.; Pan, W.; Yin, X.; Chai, P.; Pan, S.; Yang, Q. Mineralogical and Geochemical Characteristics of the Permian Coal from the Qinshui Basin, Northern China, with Emphasis on Lithium Enrichment. *Int. J. Coal Geol.* **2019**, *214*, No. 103254.
(70) Hower, J. C.; Warwick, P. D.; Scanlon, B. R.; Reedy, R. C.; Childress, T. M. Distribution of Rare Earth and Other Critical Elements in Lignites from the Eocene Jackson Group, Texas. *Int. J. Coal Geol.* **2023**, *275*, No. 104302.
(71) Sun, B.; Zeng, F.; Moore, T. A.; Rodrigues, S.; Liu, C.; Wang, G. Geochemistry of Two High-Lithium Content Coal Seams, Shanxi Province, China. *Int. J. Coal Geol.* **2022**, *260*, No. 104059.
(72) Xu, F.; Qin, S.; Li, S.; Wen, H.; Lv, D.; Wang, Q.; Kang, S. The Migration and Mineral Host Changes of Lithium during Coal Combustion: Experimental and Thermodynamic Calculation Study. *Int. J. Coal Geol.* **2023**, *275*, No. 104298.
(73) Finkelman, R. B.; Palmer, C. A.; Wang, P. Quantification of the Modes of Occurrence of 42 Elements in Coal. *Int. J. Coal Geol.* **2018**, *185*, 138−160.
(74) Hower, J. C.; Groppo, J. G.; Eble, C. F.; Hopps, S. D.; Morgan, T. D. Was Coal Metamorphism an Influence on the Minor Element Chemistry of the Middle Pennsylvanian Springfield (No. 9) Coal in Western Kentucky? *Int. J. Coal Geol.* **2023**, *274*, No. 104295.
(75) Strzałkowska, E. Rare Earth Elements and Other Critical Elements in the Magnetic Fraction of Fly Ash from Several Polish Power Plants. *Int. J. Coal Geol.* **2022**, *258*, No. 104015.
(76) Dai, S.; Seredin, V. V.; Ward, C. R.; Jiang, J.; Hower, J. C.; Song, X.; Jiang, Y.; Wang, X.; Gornostaeva, T.; Li, X.; Liu, H.; Zhao, L.; Zhao, C. Composition and Modes of Occurrence of Minerals and Elements in Coal Combustion Products Derived from High-Ge Coals. *Int. J. Coal Geol.* **2014**, *121*, 79−97.
(77) Dai, S.; Wang, P.; Ward, C. R.; Tang, Y.; Song, X.; Jiang, J.; Hower, J. C.; Li, T.; Seredin, V. V.; Wagner, N. J.; Jiang, Y.; Wang, X.; Liu, J. Elemental and Mineralogical Anomalies in the Coal-Hosted Ge Ore Deposit of Lincang, Yunnan, Southwestern China: Key Role of N2−CO2-Mixed Hydrothermal Solutions. *Int. J. Coal Geol.* **2015**, *152*, 19−46.
(78) Dai, S.; Wang, X.; Seredin, V. V.; Hower, J. C.; Ward, C. R.; O'Keefe, J. M. K.; Huang, W.; Li, T.; Li, X.; Liu, H.; Xue, W.; Zhao, L. Petrology, Mineralogy, and Geochemistry of the Ge-Rich Coal from the Wulantuga Ge Ore Deposit, Inner Mongolia, China: New Data and Genetic Implications. *Int. J. Coal Geol.* **2012**, *90−91*, 72−99.
(79) Liu, J.; Spiro, B. F.; Dai, S.; French, D.; Graham, I. T.; Wang, X.; Zhao, L.; Zhao, J.; Zeng, R. Strontium Isotopes in High- and Low-Ge Coals from the Shengli Coalfield, Inner Mongolia, Northern China: New Indicators for Ge Source. *Int. J. Coal Geol.* **2021**, *233*, No. 103642.
(80) Goldschmidt, V. M. Geochemistry. *Soil Sci.* **1954**, *78* (2), 156.
(81) Moore, T. A.; Dai, S.; Huguet, C.; Pearse, J.; Liu, J.; Esterle, J. S.; Jia, R. Petrographic and Geochemical Characteristics of Selected Coal Seams from the Late Cretaceous-Paleocene Guaduas Formation, Eastern Cordillera Basin, Colombia. *Int. J. Coal Geol.* **2022**, *259*, No. 104042.
(82) Seredin, V. V.; Dai, S. Coal Deposits as Potential Alternative Sources for Lanthanides and Yttrium. *Int. J. Coal Geol.* **2012**, *94*, 67−93.
(83) Eskenazy, G. M. On the Geochemistry of Indium in Coal-Forming Process. *Geochim. Cosmochim. Acta* **1980**, *44* (7), 1023−1027.
(84) Hower, J. C.; Berti, D.; Hochella, M. F.; Rimmer, S. M.; Taulbee, D. N. Submicron-Scale Mineralogy of Lithotypes and the Implications for Trace Element Associations: Blue Gem Coal, Knox County, Kentucky. *Int. J. Coal Geol.* **2018**, *192*, 73−82.
(85) Ribeiro, J.; Machado, G.; Moreira, N.; Suárez-Ruiz, I.; Flores, D. Petrographic and Geochemical Characterization of Coal from Santa Susana Basin, Portugal. *Int. J. Coal Geol.* **2019**, *203*, 36−51.
(86) Riley, K. W.; French, D. H.; Farrell, O. P.; Wood, R. A.; Huggins, F. E. Modes of Occurrence of Trace and Minor Elements in Some Australian Coals. *Int. J. Coal Geol.* **2012**, *94*, 214−224.
(87) Song, Y.; Liu, Z.; Gross, D.; Meng, Q.; Xu, Y.; Li, S. Petrology, Mineralogy and Geochemistry of the Lower Cretaceous Oil-Prone Coal and Host Rocks from the Laoheishan Basin, Northeast China. *Int. J. Coal Geol.* **2018**, *191*, 7−23.
(88) Huggins, F. E.; Shah, N.; Huffman, G. P.; Kolker, A.; Crowley, S.; Palmer, C. A.; Finkelman, R. B. Mode of Occurrence of Chromium in Four US Coals. *Fuel Process. Technol.* **2000**, *63* (2), 79−92.
(89) Ruppert, L.; Finkelman, R.; Boti, E.; Milosavljevic, M.; Tewalt, S.; Simon, N.; Dulong, F. Origin and Significance of High Nickel and Chromium Concentrations in Pliocene Lignite of the Kosovo Basin, Serbia. *Int. J. Coal Geol.* **1996**, *29* (4), 235−258.
(90) Zhuang, X.; Querol, X.; Plana, F.; Alastuey, A.; Lopez-Soler, A.; Wang, H. Determination of Elemental Affinities by Density Fractionation of Bulk Coal Samples from the Chongqing Coal District, Southwestern China. *Int. J. Coal Geol.* **2003**, *55* (2), 103−115.
(91) Tian, C.; Zhang, J.; Zhao, Y.; Gupta, R. Understanding of Mineralogy and Residence of Trace Elements in Coals via a Novel Method Combining Low Temperature Ashing and Float-Sink Technique. *Int. J. Coal Geol.* **2014**, *131*, 162−171.
(92) Vassilev, S. V.; Yossifova, M. G.; Vassileva, C. G. Mineralogy and Geochemistry of Bobov Dol Coals, Bulgaria. *Int. J. Coal Geol.* **1994**, *26* (3), 185−213.

https://doi.org/10.1021/acsomega.3c04109
ACS Omega 2023, 8, 39096−39109

(93) Bullock, L.; Parnell, J.; Perez, M.; Feldmann, J. Tellurium Enrichment in Jurassic Coal, Brora, Scotland. *Minerals* **2017**, *7* (12), 231.
(94) Bullock, L. A.; Parnell, J.; Feldmann, J.; Armstrong, J. G.; Henn, A. S.; Mesko, M. F.; Mello, P. A.; Flores, E. M. M. Selenium and Tellurium Concentrations of Carboniferous British Coals. *Geol. J.* **2019**, *54* (3), 1401−1412.
(95) Maksimova, M. F.; Shmariovich, Ye. M. Rhenium in Infiltration Uranium−Coal Deposits. *Int. Geol. Rev.* **1983**, *25* (2), 189−195.
(96) Yossifova, M. G. Petrography, Mineralogy and Geochemistry of Balkan Coals and Their Waste Products. *Int. J. Coal Geol.* **2014**, *122*, 1−20.
(97) Dai, S.; Seredin, V. V.; Ward, C. R.; Hower, J. C.; Xing, Y.; Zhang, W.; Song, W.; Wang, P. Enrichment of U−Se−Mo−Re−V in Coals Preserved within Marine Carbonate Successions: Geochemical and Mineralogical Data from the Late Permian Guiding Coalfield, Guizhou, China. *Miner. Deposita* **2015**, *50* (2), 159−186.
(98) Chou, C.-L. Sulfur in Coals: A Review of Geochemistry and Origins. *Int. J. Coal Geol.* **2012**, *100*, 1−13.
(99) Dai, S.; Ren, D.; Tang, Y.; Shao, L.; Li, S. Distribution, Isotopic Variation and Origin of Sulfur in Coals in the Wuda Coalfield, Inner Mongolia, China. *Int. J. Coal Geol.* **2002**, *51* (4), 237−250.
(100) Dai, S.; Hou, X.; Ren, D.; Tang, Y. Surface Analysis of Pyrite in the No. 9 Coal Seam, Wuda Coalfield, Inner Mongolia, China, Using High-Resolution Time-of-Flight Secondary Ion Mass-Spectrometry. *Int. J. Coal Geol.* **2003**, *55* (2), 139−150.
(101) Dai, S.; Ren, D.; Chou, C.-L.; Li, S.; Jiang, Y. Mineralogy and Geochemistry of the No. 6 Coal (Pennsylvanian) in the Junger Coalfield, Ordos Basin, China. *Int. J. Coal Geol.* **2006**, *66* (4), 253−270.
(102) Lindsey, D. R.; Rimmer, S. M.; Anderson, K. B. Modified Open-System Hydrous Pyrolysis. *Int. J. Coal Geol.* **2023**, *275*, No. 104313.
(103) Fikri, H. N.; Sachsenhofer, R. F.; Bechtel, A.; Gross, D. Coal Deposition in the Barito Basin (Southeast Borneo): The Eocene Tanjung Formation Compared to the Miocene Warukin Formation. *Int. J. Coal Geol.* **2022**, *263*, No. 104117.
(104) Matýsek, D.; Jirásek, J. Mineralogy of the Coal Waste Dumps from the Czech Part of the Upper Silesian Basin: Emphasized Role of Halides for Element Mobility. *Int. J. Coal Geol.* **2022**, *264*, No. 104138.
(105) Dai, S.; Zhang, W.; Seredin, V. V.; Ward, C. R.; Hower, J. C.; Song, W.; Wang, X.; Li, X.; Zhao, L.; Kang, H.; Zheng, L.; Wang, P.; Zhou, D. Factors Controlling Geochemical and Mineralogical Compositions of Coals Preserved within Marine Carbonate Successions: A Case Study from the Heshan Coalfield, Southern China. *Int. J. Coal Geol.* **2013**, *109*−*110*, 77−100.
(106) Shao, L.; Jones, T.; Gayer, R.; Dai, S.; Li, S.; Jiang, Y.; Zhang, P. Petrology and Geochemistry of the High-Sulphur Coals from the Upper Permian Carbonate Coal Measures in the Heshan Coalfield, Southern China. *Int. J. Coal Geol.* **2003**, *55* (1), 1−26.
(107) Xie, P.; Dai, S.; Hower, J. C.; Nechaev, V. P.; French, D.; Graham, I. T.; Wang, X.; Zhao, L.; Zuo, J. Nitrogen Isotopic Compositions in NH_4^+-Mineral-Bearing Coal: Origin and Isotope Fractionation. *Chem. Geol.* **2021**, *559*, No. 119946.

https://doi.org/10.1021/acsomega.3c04109
ACS Omega 2023, 8, 39096−39109